Electrochemical and Solid-State Letters, **8** (11) J30-J33 (2005)
1099-0062/2005/8(11)/J30/4/$7.00 © The Electrochemical Society, Inc.

Highly Conductive Ink Jet Printed Films of Nanosilver Particles for Printable Electronics

Dongjo Kim and Jooho Moon[z]

School of Advanced Materials Engineering, Yonsei University, Seoul 120-749, Korea

The thermal behavior of the ink-jet printed conductive films composed of Ag particles was investigated. The use of the nanosized metallic particles allows the formation of the highly conductive patterns by ink-jet printing followed by heat-treatment at temperatures much lower than the bulk melting temperature. Two different sized Ag nanoparticles were used to study the size influence on sintering temperature of the granular metal films. The resistivity variation and microstructure of the Ag films was monitored as a function of temperature using a four-point probe and scanning electron microscopy as well as thermal analysis.
 [DOI: 10.1149/1.2073670]

Manuscript submitted June 15, 2005; revised manuscript received August 1, 2005. Available electronically September 22, 2005.

The use of nanoparticles of metals with high electric conductivity provides new prospects for direct printing of conductive patterns. The microfabrication of conductive tracks by photolithographic and electroless techniques are time consuming, expensive processes, and there is an industrial need for direct digital printing to simplify the processes and to reduce manufacturing costs.[1,2] Furthermore, it is desirable to fabricate onto polymeric or similar temperature-sensitive substrates by solution-based printing process. Metallic conducting tracks of low resistance must be achieved at temperatures sufficiently lower so as to be compatible with organic electronics on plastic substrates.

Direct metal printing needs to be processed with ink materials that can convert to a low resistance conductor after solvent removal and heat-treatment. Two approaches have been pursued to attain these goals. The first is to use solutions of metallorganic precursors where the molecular nature of the compound allows low-temperature reduction to the metal.[3-5] A second route is the use of suspensions of metal particles of nanosize diameters whose small size endows a reduction in melting temperature that is significantly lower than that of the bulk material.[6-8]

The physical properties of nanoparticles are a subject of intense recent interest.[9-15] As the size of low-dimensional materials decreases to the nanometer size range, electronic, magnetic, optic, catalytic and thermodynamic properties of the materials are significantly altered from those of either the bulk or a single molecule. Especially, metal nanoparticles have very unique properties which directly relate to their dimensions and to the fact that a large ratio of the atoms in the particle are in the surface of the particle. The melting behavior of finite systems have been of considerable theoretical and experimental interest for many years, and it has been found that the melting point (T_m) of materials can be dramatically lowered by decreasing the size of the material when compared to their bulk counterparts.[9-11] Their low melting temperature, which results in low sintering temperatures, makes them potentially suitable for use in printed electronics, since they may potentially be annealed at low temperatures to form conductive films of low resistance.

In this paper, the thermal behavior of the Ag nanoparticles in the ink-jetted film is discussed. The surface microstructure and conductivity evolution of the conductive films during heat-treatment is investigated. Special emphasis is directed to compare thermal behavior of two different sized Ag nanoparticles.

Experimental

The Ag nanoparticles used were synthesized in our laboratory by the well-known polyol method. Silver nitrate (99.9%, Aldrich) used as a precursor of Ag particles was dissolved in ethylene glycol (EG, 99.9%, Aldrich) and polyvinylpyrrolidone (PVP, Aldrich) was added to protect the synthesized Ag nanoparticles from agglomeration. This solution was stirred vigorously in a reactor fitted with a reflux condenser, followed by heating to 120°C. The reaction was maintained for 30 min. After the reaction was completed, the solution was cooled to room temperature, and the silver particles were separated from the liquid by centrifugation and repeatedly washed with ethanol. The resulting particles were dried at room temperature. We prepared two different-sized Ag nanoparticles by controlling the heating rates, which were 21 ± 3 nm and 47 ± 15 nm. The synthesized Ag nanoparticles were redispersed in a mixed solvent of ethylene glycol and ethanol in a volume ratio of 5:1 together with 3 wt % PVP with respect to the dried Ag for ink-jet printing. The solid loading of the ink was 20 wt %. The formulated ink was ballmilled for 24 h, followed by filtration through a 5 μm nylon mesh. The ink has the viscosity of ~10 mPa s at shear rate of 50 s^{-1}, as measured by a cone and plate viscometer (DV – III+, Brookfield Engineering).

The Ag conductive ink was printed by an ink-jet printer onto various plastic substrates. The printer setup consisted of a drop-on-demand (DOD) piezoelectric ink-jet nozzle manufactured from Microfab Technologies, Inc. (Plano, TX) with a 30-μm orifice. The print head was mounted onto a computer-controlled three-axis gantry system capable of a movement accuracy of ±5 μm. The gap between the nozzle and the surfaces was maintained at 0.5 mm during printing at 25°C and 40% relative humidity. The uniform ejection of the droplets was performed by applying 35 V impulse lasting 20 μs at a frequency of 200 Hz. A charge coupled device (CCD) camera equipped with a strobe light emitting diode (LED) light was employed to watch an individual droplet by which the physical properties of the droplets were analyzed. The resulting Ag conductive films were heat-treated in air on a hot plate from 70 to 400°C for 30 min at a constant heating rate of 5 °C min^{-1}, and the different Ag printed films were used for each sintering temperature.

The surface morphology and the thickness of the Ag films were observed by scanning electron microscopy (SEM) (Sirion, FEI Co.). The resistivity was calculated from sheet resistance which was measured by a four-point probe (Chang Min Co., Ltd., CMT-SR200N) for the films with a 0.5 × 3000 μm cross-sectional area. A differential thermal analysis (DTA, SETARAM 90) was used for thermal profile measurement and the weight loss during heating was monitored by a thermogravimetric analyzer (TGA, SETARAM 90) and the heating rate was 5 °C min^{-1} for the thermal analysis of DTA and TGA.

Results and Discussion

Figure 1 shows various conductive patterns printed on flexible polymeric substrates including polyethylene terephthalate (PET), polyethylene naphthalate (PEN), and polyimide (PI). The diameter of the droplet and its travel velocity prior to impact were ~45.7 ± 0.5 μm and 1.2 m/s, respectively. Solvent evaporation from the printed single ink droplet produced a spherical dot pattern of ~85 μm in diameter. The line pattern was generated by narrowing the dot-to-dot distance. The separated dots started to merge together at a distance of 70 μm, whereas the printing at the condition

[z] E-mail: jmoon@yonsei.ac.kr

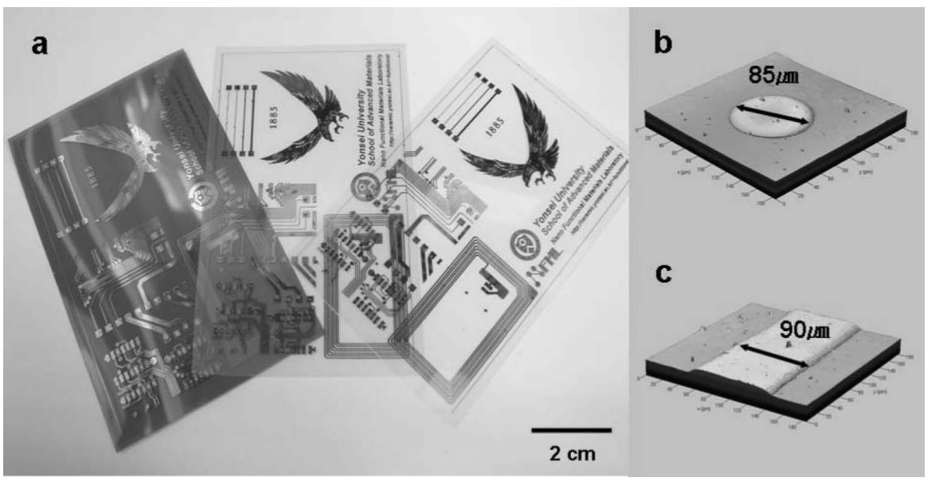

Figure 1. (a) Various ink-jet printed patterns using Ag nano particles on polymeric substrate, (b) a confocal image of the single ink droplet after drying, and (c) the printed line.

of 50 μm resulted in the continuous line with ~90 μm in width and a relatively smooth edge definition. The thickness of the resulting Ag conductive film from the single-layer printing on PI was about 0.5 μm.

The substrates of PET and PEN were distorted by heat-treatment at above 120°C due to their low glass transition temperatures. However, PI maintained the flatness up to 400°C. Because of this, we have used the PI substrate to study the conductivity variations of the silver nanoparticle films as a function of temperature. The silver films well adhered to the substrate without delamination up to 400°C. The resistivity variation of the Ag films composed of two different sized particles as a function of temperature is shown in Fig. 2a. The resistivity decreased with increasing the heat-treatment temperature, with a gradual declination at the temperate range of 100-150°C. The granular Ag films becomes relatively conductive with a resistivity of about 30 μΩ cm at 140°C for the smaller particles of 21 nm while it was at 160°C for the larger particles of 47 nm. This indicates that higher surface energy associated with smaller particles makes the film densified at lower temperatures. On the other hand, the influence of the particle size becomes insignificant when heat-treated at above 200°C. Both the Ag films made of different particle sizes exhibited similar resistivities of 3.2 μΩ cm, which was just two times higher than that of the bulk Ag (1.6 μΩ cm). The difference of the bulk conductivities may be attributed to the presence of residual organic phases such as PVP in the films and/or incomplete sintering of the particles. After a higher heat-treatment at 400°C, the conductivities of the printed Ag films became further reduced to 1.7 μΩ cm for 21 nm particles and 1.9 μΩ cm for 47 nm particles, which is close to their bulk conductivity. The different thermal behavior of the Ag films as a function of the particle size is more clearly appreciated by Arrhenius-type plotting of the electrical conductivity (σ) vs the inverse of heat-treatment temperature (Fig. 2b). In this graph, the slope of the fitted line indicates an activation energy required for the particles to be sintered. The activation energy E_a is obtained using the equation, $\sigma = \sigma_0 \exp(-E_a/kT_s)$, where k is Boltzmann's constant and T_s is the sintering temperature. The activation energy for the 21-nm particles was 0.49 eV, while 0.68 eV for the 47-nm particles, indicating higher reactivity toward sintering associated with smaller particles.

The microstructural evolution of the Ag films during the heat-treatment at temperatures ranging from 100 to 300°C is shown in Fig. 3. The films heat-treated at 100°C showed no apparent changes in particle shape and size compared with the as-synthesized particles. However, the films heat-treated at 70°C were not totally insulating. This suggests that the films have a densely packed structure in which the particles make good contact with each other. The film resistivities were observed to be rather high due to a limited area of the particle contact. It was observed that the interparticle necking occurs for the 21-nm particles fired at 140°C while at 160°C for the 47-nm particles as shown in the inserted pictures of Fig. 3b and f. These temperatures correspond to the points where the resistivity of

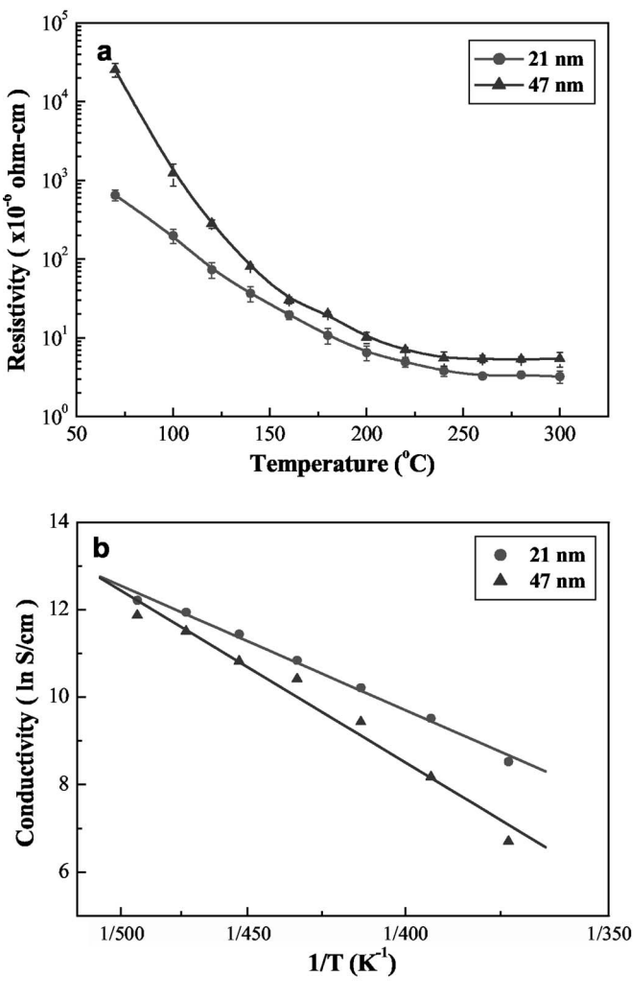

Figure 2. (a) Resistivity variation of the Ag conductive films composed of two differently sized particles as a function of heat-treatment temperature and (b) Arrhenius plot of electrical conductivity.

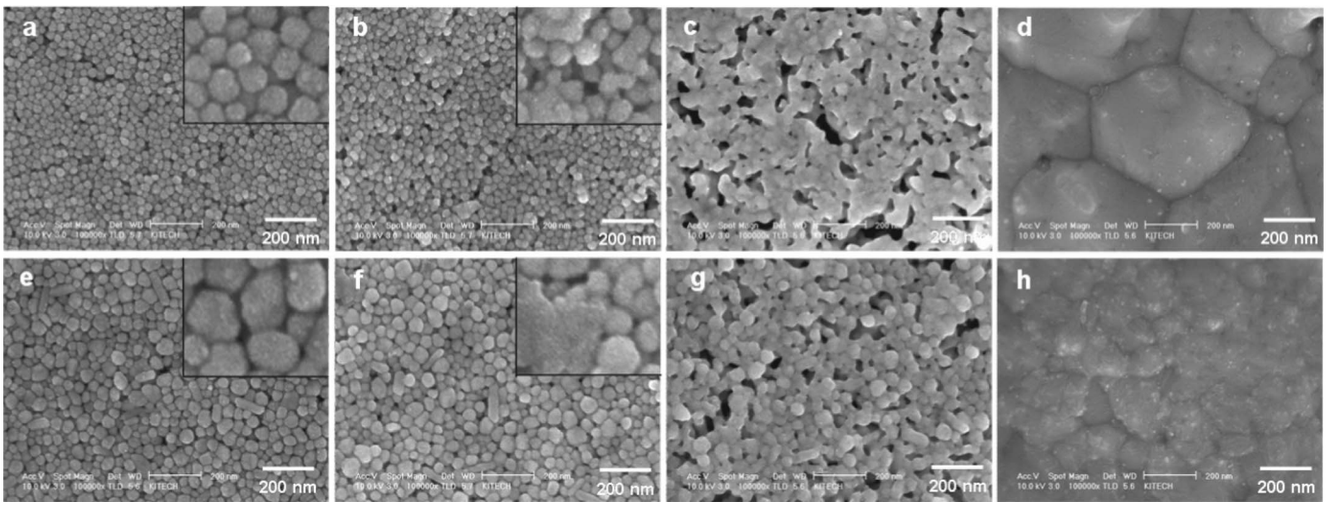

Figure 3. SEM images for microstructural variations of the Ag nanoparticle films as a function of heat-treatment temperatures. The films of 21-nm particles heat-treated at (a) 100, (b) 140, (c) 200, and (d) 300°C; the films of 47-nm particles heat-treated at (e) 100, (f) 160, (g) 200, and (h) 300°C.

each film exhibit relatively low values of about 30 $\mu\Omega$ cm. To be such a conductive layer from the nearly insulating particulate films, the granular film needs to have a three-dimensionally interconnected conduction pathway, which requires, to some extent, interparticle neck growth. In this regard, it is believed that the temperatures at which the interparticle necking occurs are at around 140°C for the 21-nm particles and 160°C for the 47-nm particles. The films heat-treated at above 200°C show dramatic changes in the particle shape from discrete and spherical particles to continuous and sintered particles. Heat-treatment at higher temperatures densifies the films accompanying grain growth and volumetric shrinkage. These microstructural observations clearly demonstrate that the neck formation is responsible for providing a continuous pathway for the electronic conduction. Once the particle necking with sufficient interparticle neck size is formed, the granular Ag films become relatively well conductive even though it is still porous. Further densification does not bring about a significant increase in the conductivity, which is consistent with the percolation theory.[16,17]

The TG/DTA results for the Ag nanoparticles dried from the conductive ink are shown in Fig 4. There exists a continuous weight loss at the temperatures ranging from 100 to 500°C (Fig. 4). Since the organic additive PVP used in formulating the ink decomposes around 400°C, it is believed that the weight loss around 200°C is from the removal of residual solvents, rather than from the burn-out of the organic materials. Therefore, it is considered that all the Ag films heat-treated at below 300°C contained the residual organic phases. Because of this, the resistivity of the film sintered at 300°C was two times higher than the bulk resistivity as shown in Fig. 2a. The exothermic peaks are also observed in the DTA analysis at the temperature between 100-200°C. The peak for the 21-nm particles is located at 120°C whereas it is at 160°C for the 47-nm particles (Fig. 4). The peak positions match relatively well with the temperatures where the resistivities of the films are relatively low ($\sim$30 $\mu\Omega$ cm) and where the interparticle neck growth occurs.

The exothermic peaks can be attributed to the crystallization of amorphous metal particles or recrystallization of strained metal particles upon heating. Since our particles are phase-pure well-crystalline Ag, however, these possibilities can be eliminated. It is also reported that surface diffusion of unstable atoms on the nanoparticles during their neck formation can generate the exothermic peaks.[18] If so, the exothermic peak position should be correlated with the particle size. The smaller particles involve unstable surface atoms at higher energy states, which can undergo sintering at temperature lower than the larger particles as we found in the DTA. Our

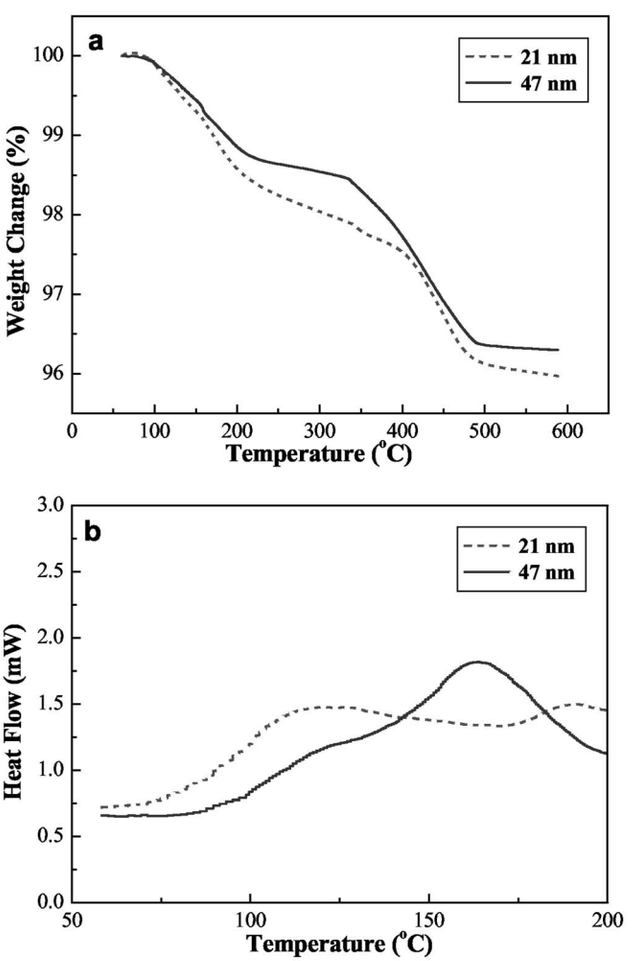

Figure 4. TG and DTA curves of the Ag particles used in the preparation of the conductive ink.

thermal analysis is in good agreement with the conductivity variation of the Ag nanoparticle films prepared from two different particle sizes as a function of heat-treatment temperature concurrent with the corresponding microstructural evidence.

Conclusions

We have demonstrated a direct metal printing of the Ag nanoparticles on plastic substrates. The granular Ag films become highly conductive, $\sim$3.2 $\mu\Omega$ cm, when heat-treated even at 200°C. Thermal behavior of the granular Ag films was investigated with respect to the conductivity variation and the film microstructure. The Ag particles of smaller size are more reactive than the larger sized particles in which the interparticle neck forms at temperature $\sim$140°C. Heat-treatment at higher temperatures makes the neck size grow by further densification, resulting in a gradual increase in the conductivity of the films. Conductivity variations of the Ag film are well correlated with morphological evolution of the microstructure as well as thermal analysis.

Acknowledgments

This work was supported by National Research Laboratory Program from Korea Science and Engineering Foundation.

Jooho Moon assisted in meeting the publication costs of this article.

References

1. D. Huang, F. Liao, S. Molesa, D. Redinger, and V. Subramanian, *J. Electrochem. Soc.*, **150**, G412 (2003).
2. A. Kamyshny, M. Ben-Moshe, S. Aviezer, and S. Magdassi, *Macromol. Rapid Commun.*, **26**, 281 (2005).
3. A. L. Dearden, P. J. Smith, D.-Y. Shin, N. Reis, B. Derby, and P. O'Brien, *Macromol. Rapid Commun.*, **26**, 315 (2005).
4. Y. Byun, E.-C. Hwang, S.-Y. Lee, Y.-Y. Lyu, J.-H. Yim, J.-Y. Kim, S. Chang, L. S. Pu, and J. M. Kim, *Mater. Sci. Eng., B*, **117**, 11 (2005).
5. G. G. Rozenberg, E. Bresler, S. P. Speakman, C. Jeynes, and J. H. G. Steinke, *Appl. Phys. Lett.*, **81**, 5249 (2002).
6. S. B. Fuller, E. J. Wilhelm, and J. M. Jacobson, *J. Microelectromech. Syst.*, **11**, 54 (2002).
7. J. Chung, S. Ko, N. R. Bieri, C. P. Grigoropoulos, and D. Poulikakos, *Appl. Phys. Lett.*, **84**, 801 (2004).
8. S. Molesa, D. R. Redinger, D. C. Huang, and V. Subramanian, *Mater. Res. Soc. Symp. Proc.*, **769**, H8.3.1 (2003).
9. P. Buffat and J-P. Borel, *Phys. Rev. A*, **13**, 2287 (1976).
10. G. L. Allen, R. A. Bayles, W. W. Gile, and W. A. Jesser, *Thin Solid Films*, **144**, 297 (1986).
11. Q. Jiang, S. Zhang, and M. Zhao, *Mater. Chem. Phys.*, **82**, 225 (2003).
12. C. Herring, *J. Appl. Phys.*, **21**, 301 (1950).
13. J. G. Dash, *Rev. Mod. Phys.*, **71**, 1737 (1999).
14. K. Dick, T. Dhanasekaran, Z. Zhang, and D. Meisel, *J. Am. Chem. Soc.*, **124**, 2312 (2002).
15. Z Zhang, J. C. Li, and Q. Jiang, *J. Phys. D*, **33**, 2653 (2000).
16. G. E. Pike and C. H. Seager, *Phys. Rev. B*, **10**, 1421 (1974).
17. S. K. Mandal, A. Hangopadhyay, S. Chaudhuri, and A. K. Pal, *Vacuum*, **52**, 485 (1999).
18. K.-S. Moon, H. Dong, R. Maric, S. Pothukuchi, Y. Li, and C. P. Wong, *J. Electron. Mater.*, **34**, 168 (2005).